Available online at www.sciencedirect.com

ScienceDirect

IFAC PapersOnline CONFERENCE PAPER ARCHIVE

IFAC PapersOnLine 55-9 (2022) 87–92

Solar microsystem modeling and simulation: photovoltaic inverter control based on energy technical product quality criteria

F. Grau*, L. Vazquez*, J. Cervantes*, Y. Majanne**

**Electrical Engineering Faculty, University of Oriente, Ave. Las Americas s/n, 90400 Santiago of Cuba, Cuba (e-mail: fgrau@uo.edu.cu, lvazquez@uo.edu.cu, lvazquez0211@gmail.com, janette@uo.edu.cu)*

*** Faculty of Engineering and Natural Sciences, Tampere University, P.O. Box 541, FI-33014 Tampere University, Finland (e-mail: yrjo.majanne@tuni.fi))*

Abstract: In this work an analysis of the quality of electric power in off-grid solar photovoltaic microsystems is carried out. Applied to an existing case study in an island developing country like Cuba, the purpose is to control the bridge inverter to reduce the effect of harmonics. The tripping of the switches is controlled by pulse width modulation (PWM). The design is computer aided with Simulink / Matlab. The testing of different control strategies in these systems resulted proposing the design method of a Proportional - Resonant controller control system. The results with an isolated single-phase system with a residential load reveal the reduction of the total harmonic distortion (THD) in the voltage at the output of the solar PV inverter filter to the AC load.

Keywords: power quality; photovoltaic solar system, THD; inverter; PWM, Proportional –Resonant control.

1. INTRODUCTION

The electricity market is increasingly demanding in terms of the quality of the service supplied, not only an uninterrupted electricity supply is required, but it must also be guaranteed that the values of the quality parameters should be within the ranges established for the different voltage zones. These requirements are part of the "Quality of Electrical Energy" and, in Cuba, the set of indicators describing the waveform of voltages and currents is known as Technical Product Quality indicators (Barandiaran, et al., 1991). The definition of the term is not unique and varies from country to country.

On the other hand, the use of Renewable Energy Sources (RES) in Distributed Generation (DG) responds to the country's policy of transforming the energy matrix as part of the Sustainable Development Goals (SDGs) for 2030 (Mondejar, et al, 2021, Sagastume et. al, 2018). In Cuba, it is expected that RES will occupy 24 % of the energy matrix and solar photovoltaic (PV) generation will be 3 % of the total generated energy. It will reach 700 MWp of installed capacity by 2030 (Vazquez, et. al 2018, Singh, 2020).

In PV systems, the waveforms of current and voltage signals deteriorate for several reasons, among them the nonlinearity of the loads and the distortion in the waveform of the voltages at the inverter output, caused by conversion from Direct Current (DC) to Alternating Current (AC) (Carbonell, et. al, 2014, Trapanese, et. al. 2014).

When a modification of the installation is not possible or it is very expensive, it is common to employ passive, active or hybrid filters on the elements of the load that have higher contribution to the distortion. However, in solar PV systems equipped with inverter control or multilevel inverters with a specific connection architecture, (Abdelwahab, et al., 2018) it is possible to improve the quality of voltage and current signals.

The Proportional - Integral (PI) control algorithm shows insufficiencies when trying to achieve zero steady state error for systems with low order harmonics and when the switching frequency is reduced (Ortega, et. al. 2016). PI controllers are usually not employed in solar PV inverters as a part of the current control loop. The alternative adopted in these cases is the Proportional - Resonant (PR) controller (Castilla, et. al. 2013).

2. SCHEME FOR CONTROL SYSTEM DESIGN

PV generation in isolated microsystems (μSPV) is feasible for power supply in rural residential distribution networks, operating in an islanded mode or together with other generation sources.

It is possible to develop control schemes with low computational load that are capable to control PV generation in distribution networks. For the control system design, a μSPV (micro Solar-PV) simplified scheme is shown in Figure 1 (Mera, 2019). The fundamental elements of the system are: solar PV array (PV Array), DC bus (DC Link), DC - AC converter (Inverter), a filter at the inverter output (LCL Filter), whose purpose is to control the current injected to the system so that the higher order harmonics shall be attenuated, the linear and nonlinear load (Load) and the inverter control module (PWM Control). The inverter is implemented from an array of semiconductor elements connected in a bridge configuration, using insulated gate bipolar transistors (IGBT). The inverter is controlled by pulse width modulation (PWM). The control signal is constructed from the setpoints of voltages and currents in the DC and AC Bus producing the modulation index at which the PWM generator is operated.

The use of tuned PR controllers has been described in PV applications (Abdelwahab, et al., 2018), and in wind and hydro power generation (Castilla, 2013, Zmood, 2001, Yuan, et. al,

10.1016/j.ifacol.2022.07.016

2002, Zmood , et. al, 2003, Liserre, et. al., 2006, Shen, et.al, 2010, Lee, et.al., 2011 and Castilla, et. al, 2009).

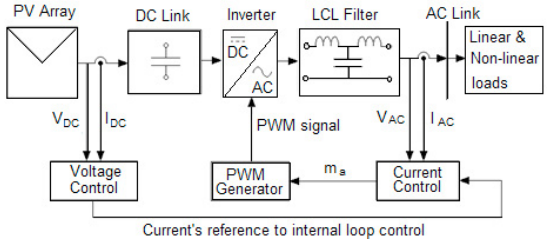

Figure 1. A simplified μSPV scheme for control system design.

The fundamental advantage of PR controllers is in harmonic cancellation and the possibility to supply reactive control in the system. This is made possible by their ability to tune a given frequency of a sinusoidal signal with zero error in a steady state (Ortega, et. al. 2016, Zmood, et. al, 2003). A drawback of this type of controller is the fact that it is affected by abnormal network operating conditions, such as voltage and current unbalance in three-phase systems and harmonic components of the currents demanded by the network (Ortega, et. al. 2016). In general, with PR algorithm it is possible to design control schemes with low computational effort with capability to control PV inverters in distribution networks.

3. CONTROL SYSTEM DESIGN METHOD

The simulation model of the μSPV is defined and parameterized based on the data from the isolated μSPV of the province of Santiago de Cuba, Cuba. The system is installed in the Rural Community Santa María del Loreto. The distribution system is composed of two radial circuits of secondary distribution at low voltage (230V), Santa María del Loreto 1 and 2, with lengths of 1.84 km and 2.27 km respectively. The PV farm has a nominal output power of 8 kWp. It consists of 90 units of 110 W ATERSA panels, and 48 units of 150 W ISOFOTÓN panels. There is also a 3,600 Ah Tudor battery bank. Both circuits ae powered by 4 kWp Tauro inverters. Modelling data has been logged from the μSPV Santa Maria del Loreto 1, which feeds 20 homes, a doctor's office, a coffee pulper, a store and a school. The data for system design is presented in Table 1.

Table 1. Data from the μSPV Santa María del Loreto 1.

Magnitudes	Symbols	Values
Power of the load	P_L	3500 W
Rated voltage	V_{LN}	230 V
Rated current	I_{LN}	14,58 A
Frequency	f_0	60 Hz
Switching frequency	$f_{s\omega}$	10 kHz
DC bus voltage	V_{CD}	400 V

DC bus design

The DC bus applies an input capacitor in front of the inverter. Ripple in the DC voltage signal (V_{DC}) can cause considerable power losses. The capacitor must be capable of filtering higher order harmonic components (Castilla, 2013, Mera, et. al. 2019). The capacitance of the input capacitor C_{DC} is:

$$C_{DC} = \frac{P_{FV}}{2\omega V_{DC}\Delta V_{DC}}, \quad (1)$$

where C_{DC} is the capacitor on the direct bus, P_{FV} is the power of the photovoltaic array, ω is the frequency of the network, V_{DC} is the input voltage to the inverter, ΔV_{DC} is the allowed or desired ripple value on the DC Bus (for the design $\Delta V_{DC} = 0{,}1 \cdot V_{DC}$). Using the data provided in Table 1, a capacitor of 5,8 μF is obtained.

LCL Filter Design

The LCL filter attenuates the higher order harmonics of the current fed into the system. The objective is to adjust the filter to a cut-off frequency equal to that of the mains. In practice it must be considered that these filters have a high quality factor resulting to a low damping for frequency values equal to those of the cut-off frequency. For this reason a series resistor *Rd* is added to the capacitor branch in order to increase the damping and increase the stability in the system. (Mera, 2019, Patiño, et. al. 2012, Castro, et. al. 2014, Tiwari et. al. 2010, Avila, et. al., 2011 and Villa, 2011). The LCL filter scheme is shown in the Figure 2.

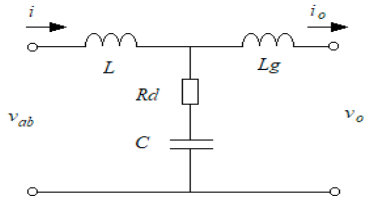

Figure 2. LCL filter with damping resistance *Rd*.

The transfer function of the filter is:

$$H_o(s) = \frac{I_o(s)}{V_{ab}(s)} = \frac{(R_d C s+1)}{LL_g C s^3 + R_d C(L+L_g)s^2 + (L+L_g)s} \quad (2)$$

In this transfer function, the cut-off frequency is:

$$\omega_0 = \sqrt{\frac{L+L_g}{LL_g C}} \quad (3)$$

The tailored values are summarized in Table 2:

Table 2. Filter design values at the inverter output.

Magnitudes	Symbols	Values
Input inductance	L	2,28 mH
Output inductance	Lg	2 mH
Capacitor	C	8 μF
Damping resistor	R_d	3,48 Ω

Inverter control scheme design

The block diagram supported in LTI (Linear Time Invariant) modeling technique for standard inverter control consists of two loops, an outer loop for AC bus voltage control and an inner loop for output current control of the LCL filter (Mera,

2019). The structure of the model is shown in Figure 3.

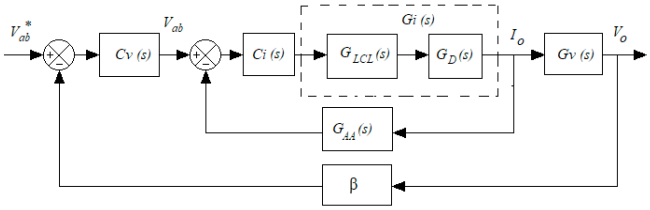

Figure 3. LTI based modeling for PV inverter control on generation distribution networks.

Table 3 defines the blocks of the scheme in Figure 3 (Kanieski, et. al, 2010, Ortega, et. al, 2016, IEC, 2002).

The current controller C_i maintains the active and reactive power levels on the AC bus. The loop must be designed to ensure a dynamic steady-state response that is faster than that of the voltage loop.

Table 3. PV inverter control scheme blocks.

Blocks	Symbols
Voltage plant	$G_v(s)$
Current plant	$G_i(s)$
Voltage controller	$C_v(s)$
Current controller	$C_i(s)$
LCL Filter Transfer Fcn.	$G_{LCL}(s)$
Smith Predictor	$G_D(s)$
Anti-aliasing filter	$G_{AA}(s)$
Voltage transducer gain	β

It is desired to produce a sinusoidal voltage waveform in the inverter output maintaining constant amplitude and frequency of voltage signal. Nevertheless, due to the presence of nonlinear loads with high levels of distortion with the current signal, it is difficult to reach this sinusoidal behavior (IEC, 2002). A solution is a PR controller. The controller characteristic equation is as follows (Ortega, et. al. 2016):

$$C_{PR}(s) = K_P + \frac{K_i 2\xi\omega_0 s}{s^2+2\xi\omega_0 s+{\omega_0}^2} \quad (4)$$

where: K_P is the proportional gain of the controller, K_i is the integral gain, ξ is the harmonic damping coefficient, ω_0 is the cutoff frequency corresponding to the fundamental harmonic (f_0 = 60 Hz).

This paper considers the PR controller composed by a proportional gain plus a resonant controller $K_P + C_{RES}(s)$. The resonant controller $C_{RES}(s)$ is considered as a harmonic controller, when its frequencies are multiple of the fundamental system's frequency. The proportional gain (K_P) is added to the resonant controller in order to introduce a high frequency gain in the current loop cancelling the disturbances at the output. The general expression of the controller $C_i(s)$ is:

$$C_i(s) = K_P + C_{RES}(s) \quad (5)$$

The value of the proportional gain (K_P) is determined by the expression:

$$K_P = \frac{(L+Lg)\cdot\omega_{Ci}}{R_i\cdot F_m\cdot 2\cdot V_{DC}} \quad (6)$$

where (L+Lg) is the inductance seen at the inverter output, ω_{ci} is the current loop cutoff frequency (desired), R_i is the gain of the current sensor (Ri = 0,2), F_m is the gain of the bipolar PWM modulator, and V_{DC} is the voltage on the DC bus. Half of the inverter switching frequency is used to determine this value:

$$\omega_{Ci} = 2\pi\frac{f_{s\omega}}{2}, \quad (7)$$

The value of F_m is determined as:

$$F_m = \frac{1}{V_{pp\_tri}}, \quad (8)$$

where V_{pp_tri} is the peak-to-peak voltage of the triangular signal (modulating signal Vtri).

On the other hand, the resonant controller $C_{RES}(s)$ can be described as a second order filter whose transfer function is given by the expression:

$$C_{RES}(s) = \frac{K_h\cdot B_h\cdot s}{s^2+B_h s+(\omega_h)^2}, \quad (9)$$

where K_h is the gain of the resonance peak at frequency ω_h, ω_h is the pulsation of the resonance multiple of the fundamental frequency ω_0, in such a way that $\omega_h = h\cdot 2\pi f$, and B_h is the bandwidth expressed in rad/s.

According to the design elements of the current loop and considering a value of h = 1 (fundamental frequency), K_h = 100, B_h = 2π we obtain that the Proportional - Resonant controller will have the following transfer function:

$$C_i(s) = 0{,}84 + \frac{100\cdot 2\pi\cdot s}{s^2+2\pi s+(2\pi 60)^2} \quad (10)$$

Figure 4 shows that the current loop response with the designed controller is 35,9 dB. The phase shift value for this frequency is -5°, which corrects the phase shift of -90° obtained in the response without controller.

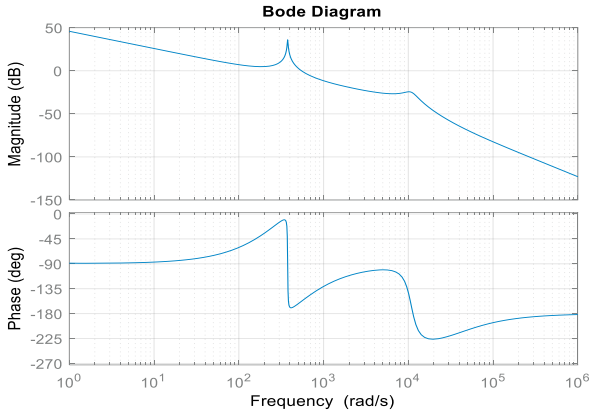

Figure 4. Current loop response with PR controller.

Once the elements of the current control loop have been calculated, it is possible to calculate the voltage control loop.

In Figure 3, the block β represents the gain of the voltage sensor (β=0,006). The plant transfer function for the voltage Gv(s) is composed of a function $G_{load}(s)$ which is obtained from the ratio between the load current (I_o) and the voltage on the AC bus

(V_o). This ratio corresponds to the load impedance, which for controller design purposes will be considered pure resistive.

$$G_{load}(s) = \frac{V_o(s)}{I_o(s)} = R_o = \frac{V_{oN}}{I_{oN}}, \quad (11)$$

where R_o represents the load connected to the inverter output and can be calculated from the design elements in Table 1.

The closed-loop transfer function without the controller is:

$$H(s) = \frac{G_v(s)}{1+\beta \cdot G_v(s)} = \frac{0{,}2571s+16{,}48}{243{,}4\cdot 10^{-6}s^2 + 0{,}03274\ s + 1{,}099} \quad (12)$$

To correct the dynamic response, it is necessary to dimension a controller capable of restoring the response value in a time less than twice the period of the fundamental signal. For this purpose, a Proportional - Integral (PI) controller can be used.

$$C_v(s) = K_P + \frac{K_i}{s} = \frac{K_P s + K_i}{s}, \quad (13)$$

The PI controller design is performed based on two basic criteria, the maximum overshoot (M_p) and the settling time (T_{ss}) (Ortega, et. al., 2016). The settling time has been selected less than or equal to $\frac{1}{3}$T (5,55·10^{-3} s) and the overshoot will be set at 10%. The controller is tuned by using the pole assignment method. The transfer function of the controller is:

$$C_v(s) = 236{,}886 + \frac{255{,}3\cdot 10^3}{s} \quad (14)$$

System modeling and simulation

The Simulink/Matlab model of the system consist of PV Array blocks, the Universal Bridge inverter, and the PWM Generator. The PV Array setup consists of 4 modules in parallel, each with 24 panels in series with a maximum power 250,2 W and a voltage at the MPP point of 30,7 V.

Functional blocks belonging to the CD bus, LCL filter and load are used in the simulation, which are implemented from RLC branches. Other functional blocks are used as constant inputs, voltage and current meters, signal bus, multiplexers and demultiplexers, oscilloscopes, displays and blocks to determine the spectrum of the output signal by means of its decomposition in the Fourier series. A phase tracking loop (PLL) block is used to determine the frequency. Figure 5 shows the model.

4. ANALYSIS AND EVALUATION OF RESULTS

The RMS value of the voltage that is proportional to the amplitude of the fundamental harmonic is selected as a quality indicator. Another important indicator is the Total Harmonic Distortion value of the voltage (THD).

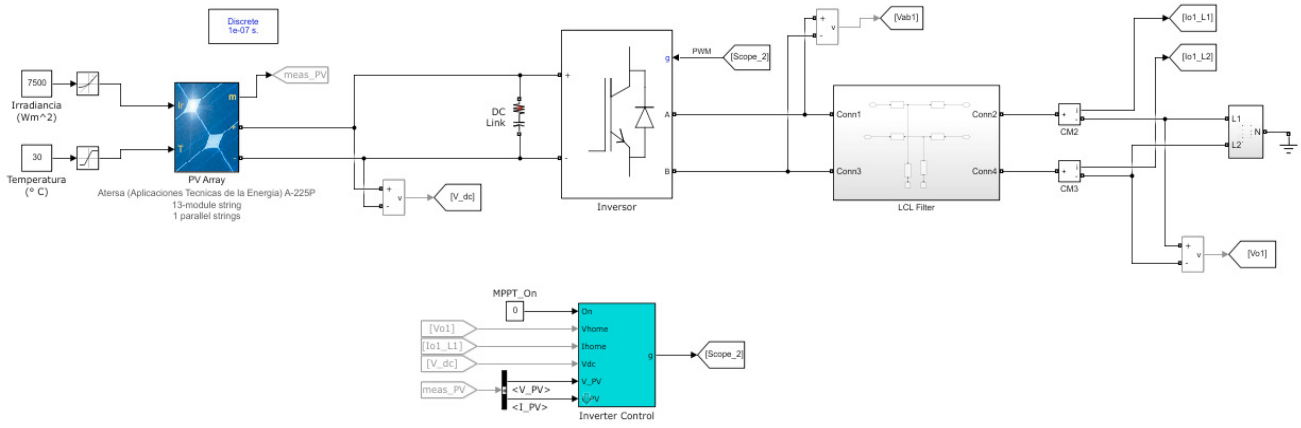

Figure 5. Simscape model of the µSPV Santa María del Loreto 1.

The control scheme is also implemented in Matlab/Simulink. The values used in each of the functional blocks are in Table 4.

Table 4. Discretization of the functional blocks of the control model.

Functional block	Transfer function	Z – Transform
$G_i(s)$	$e^{-10^{-5}s} \cdot \frac{3{,}078\cdot 10^{-5}s+1}{3{,}648\cdot 10^{-11}s^3+1{,}317\cdot 10^{-7}s^2+0{,}00428s}$	$z^{-1} \cdot \frac{4{,}616\cdot 10^{-5}z^2+1{,}743\cdot 10^{-5}z-6{,}67\cdot 10^{-5}}{z^3-2{,}953z^2+2{,}918z-0{,}9645}$
$G_{AA}(s)$	$\frac{1{,}508\cdot 10^4}{s^2+1{,}508\cdot 10^4 s+2{,}274\cdot 10^8}$	$\frac{7{,}161\cdot 10^{-7}z+6{,}81\cdot 10^{-7}}{z^2-1{,}839z+0{,}86}$
$C_i(s)$	$0{,}84 + \frac{100\cdot 2\pi\cdot s}{s^2+2\pi s+(2\pi 60)^2}$	$\frac{0{,}84z^2+1{,}68z+0{,}8399}{z^2-2z+0{,}9999}$
$G_v(s)$	$\frac{16{,}48}{0{,}0156s+1}$	$\frac{0{,}01056}{z-0{,}9994}$
$C_v(s)$	$236{,}886 + \frac{255{,}3\cdot 10^3}{s}$	$\frac{236{,}9z-234{,}3}{z-1}$

The simulation results show a harmonic distortion for the voltage of 8,17%, which is slightly higher than the recommended value of a THDv = 8%, according to the IEC 61000-2-2 Standard (IEC, 2002). The harmonics of the currents are 9,33% for line 1 and 10,37% for line 2, Table 5.

Table 5. Microsystem simulation results without controller.

Magnitudes	THD (%)	CF	RMS
V_{o1}	8,17	1,65	230 V
I_{oL1}	9,33	1,597	14,81 A
I_{oL2}	10,37	1,641	13,34 A

Results of the system simulation using a Proportional - Resonant current controller

In Figure 6, the output voltage without the PR controller is shown in blue and with the PR controller (red). It is noticed that the system stabilization time does not exceed the two periods of the signal. To decrease stabilization time and stationary error, an integral proportional controller can be implemented for the voltage control loop.

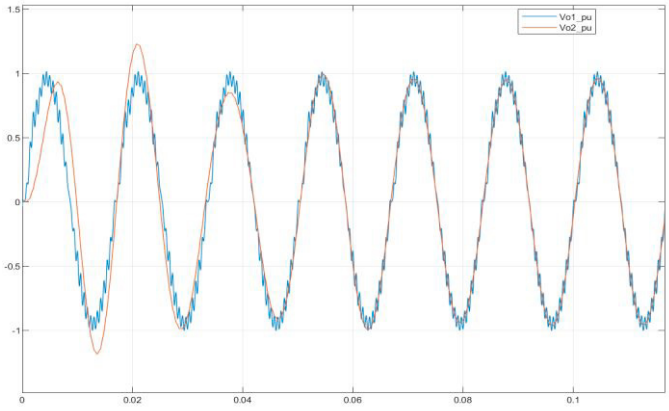

Figure 6. Simulation results by a PR controller on μSPV Santa María del Loreto 1.

The spectrum analysis of the output voltage shows that the individual harmonics 6 and 8 are above the normalized value (0,5%), as well as the harmonic of order 27 (0,2%). These components are highlighted in red in Figure 7 (a). In the case of the implementation of the PR controller, none of the components of the spectrum exceeds the normalized value (Figure 7 (b)).

Table 6 summarizes the main results for electrical voltage. The table shows that the amplitude and phase values for the fundamental harmonic are very similar, whereas the results obtained with the proportional resonant controller reveals that the signal does not have a harmonic content or significant ripple, unlike the signal without a driver.

The simulation results reveal how the use of current control by a PR controller reduces the THD in the input signal while ensuring similar voltage deviation values. The fundamental difference in terms of the effective value of the signal is given precisely by the elimination of harmonics present in the signal at the output of the filter without a controller.

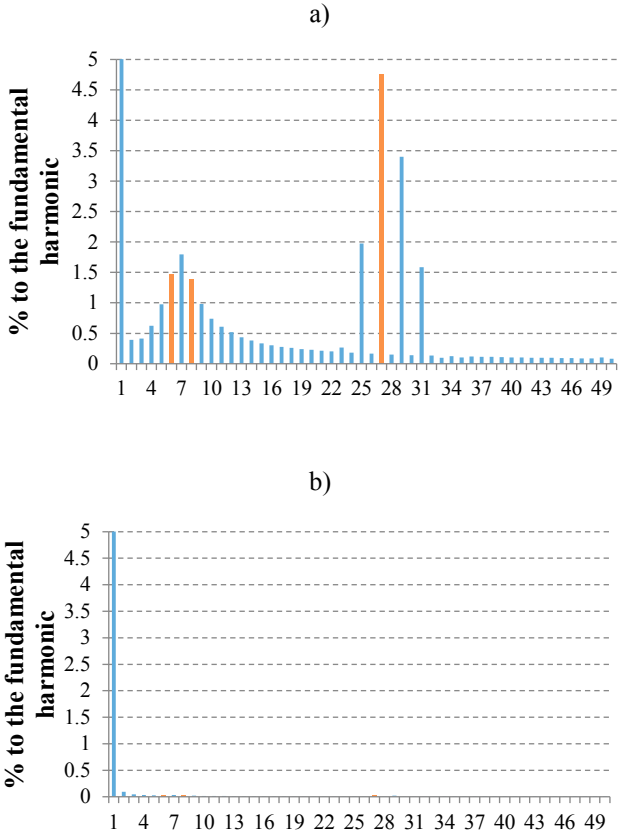

Figure 7. Harmonics of the voltage signal at the output: a) No controller. b) With PR controller.

Table 6. Results of the voltage signal analysis.

Indicators	V_{o1} (without Ci controller)	V_{o2} (with Ci controller)
Amplitude (V)*	324,1	324,8
Fase (°)*	-7,32	-6,642
RMS	230	229,6
ΔV (%)	-4,2	-4,3
CF	1,65	1,41
THD (%)	8,17	0,6

(*) The amplitude and phase values refer to the fundamental harmonic

5. CONCLUSIONS

The adequate design of the output filter, the selection of the modulation indices for the PWM control of the inverter, and the use of current controllers, such as the PR controller, guarantee levels of harmonic distortion and voltage deviation within the permissible ranges according to the standards governing the quality control of the technical product in facilities isolated from the network. The design of a Proportional - Resonant controller for the current control loop in the simulation of the isolated microsystem Santa María del Loreto 1 resulted a reduction of the THD in the voltage from 8% to 0,6%, improving the quality of the voltage waveform without worsening of other quality indicators of the system.

ACKNOWLEDGEMENTS

This contribution is a result of the Power Electronics Control in Energy and Motion Systems group (PECEM) in the

Electrical Engineering Faculty from University of Oriente, Santiago de Cuba in cooperation with Tampere University in Finland. The work was supported by the IRIS project (Cuban energy transformation. Integration of Renewable Intermittent Sources in the power system, 2019-2022) financed by the Academy of Finland, Grant/Award Number 320229. The authors of the article gratefully acknowledge the financers and project partners.

REFERENCES

H. Abdelwahab, et al., (2018) Harmonic Reduction for Grid-Connected PV System based on Multilevel Inverter, Australian Journal of Basic and Applied Sciences, 12 (9), pp. 135-145,

Deivis Ávila, et. al., (2011). Sistemas híbridos con base en las energías renovables para el suministro de energía a plantas desaladoras, Ingeniería Mecánica. Vol. 14. No. 1, enero-abril.

J. Barandiaran, I. Laresgoiti, J. Pérez, J. Corera, J. Echávarri, (1991). An Expert System for the Analysis of Disturbances in Electrical Networks, Operational Expert System Applications in Europe, pp. 145-166.

T. Carbonell, et. al (2014), Hydrogen from Renewable Energy in Cuba, Energy Procedia, 57, pp. 867-876,

M. Castilla, et. al (2009), Control design guidelines for single-phase grid-connected photovoltaic inverters with damped resonant harmonics compensators, in IEEE Trans. Ind. Electron., 56 (11), (2009), pp. 4492–4501.

M. Castilla, et.al. (2013). Reduction of Current Harmonic Distortion in Three-Phase Grid-Connected Photovoltaic Inverters via Resonant Current Control, in IEEE Transactions on Industrial Electronics, 60 (4), pp. 1464-1472.

Ospino Castro, et. al. (2014), Modelado y simulación de un panel fotovoltaico empleando técnicas de inteligencia artificial, Revista Energética, vol.35 no.3 La Habana.

IEC 61000-2-2, (2002). Environment – Compatibility levels for low-frequency conducted disturbances and signalling in public low-voltage power supply system

Kanieski, Joao Marcos; Scapini, Rafael (2010), Influences of the Anti-Aliasing Filter Damping Factor in an Active Power Filtering Environment, Universidade Tecnologica Federal do Paraná, ResearchGate, Conference paper.

T. L. Lee, et.al., (2011). Resonant current compensator with enhancement of harmonic impedance for LCL-filter based active rectifiers, in Proc. IEEE APEC, pp. 1538–1543.

M. Liserre, R. Teodorescu, and F. Blaabjerg, (2006) "Multiple harmonics control for three-phase grid converter systems with the use of PI-RES current controller in a rotating frame, in IEEE Trans. Power Electron., 21 (3), pp. 836–841

Intriago Mera, Otto Fernando (2019), Diseño y Simulación de un Inversor para Energía Solar Fotovoltaica Adaptativo con Vertido Cero a Red, Universidad de Alcalá, Escuela Politécnica Superior, http://hdl.handle.net/10017/39866

M. E. Mondejar, et al.(2021), Digitalization to achieve sustainable development goals: Steps towards a Smart Green Planet. Science of The Total Environment, 794, pp. 148539,

R., Ortega, O. Carranza, J. Soza, (2016). Diseño de controladores para inversores monofásicos operando en modo isla dentro de una microred, Revista Iberoamericana de Automática e Informática Industrial (RIAII), pp. 115- 126.

Sebastián Patiño, et. al. (2012), Diseño e implementación de un sistema fotovoltaico híbrido y desarrollo de su regulador de carga aplicando instrumentación virtual, Departamento de Ingeniería Eléctrica, Universidad Distrital Francisco José de Caldas, Bogotá, Colombia.

A. Sagastume, J. J. Cabello Eras, D. Huisingh, C. Vandecasteele, L. Hens (2018), The current potential of low-carbon economy and biomass-based electricity in Cuba. The case of sugarcane, energy cane and marabu as biomass sources, Journal of Cleaner Production, 172, pp. 2108-2122,

G. Shen, et.al, (2010). A new feedback method for PR current control of LCL-filter-based grid-connected inverter, in IEEE Trans. Ind. Electron., 57 (6), , pp. 2033–2041.

B. Singh, et. al, (2020). Power Quality Improvement of Grid Connected PV System, IEEE India Council International Subsections Conference (INDISCON), pp. 188-194.

Tiwari, G.; Dubey, S. (2010), Fundamentals of Photovoltaic Modules and Their Applications, 2da. ed., United Kingdom: RSC Publishing, 402 p.

M. Trapanese, A. Viola (2019), Small Island developing states: Overview about wind, solar and marine energy in Cuba, OCEANS 2019 MTS/IEEE SEATTLE, pp. 1-6.

X. Yuan, et. al (2002), Stationary-frame generalized integrators for current control of active power filters with zero steady-state error for current harmonics of concern under unbalanced and distorted operating conditions, in IEEE Trans. Ind. Appl., 38 (2), pp. 523–532.

D. N. Zmood, D. G., et. al. (2001), Frequency-domain analysis of three-phase linear current regulators, in IEEE Trans. Ind. Appl., 37 (2), (2001) pp. 601–610.

D. N. Zmood and D. G. Holmes, (2003). Stationary frame current regulation of PWM inverters with zero steady-state error, in IEEE Trans. Power Electron., 18 (3), pp. 814–822.

Villa Manrique, Alberto (2011), Estudio del Filtro LCL aplicado a Inversores Fotovoltaicos, Departamento de Ingeniería Eléctrica, UC3M, Madrid.

L. Vázquez, et al. (2018), Energy System Planning towards Renewable Power System: Energy Matrix Change in Cuba by 2030, IFAC PapersOnLine, 51 (28), pp. 522–527.